

# Making silole photovoltaically active by attaching carbazolyl donor groups to the silolyl acceptor core†

Baoxiu Mi,<sup>a</sup> Yongqiang Dong,<sup>a</sup> Zhen Li,<sup>a</sup> Jacky W. Y. Lam,<sup>a</sup> Matthias Häußler,<sup>a</sup> Herman H. Y. Sung,<sup>a</sup> Hoi Sing Kwok,<sup>a</sup> Yuping Dong,<sup>a</sup> Ian D. Williams,<sup>a</sup> Yunqi Liu,<sup>c</sup> Yi Luo,<sup>d</sup> Zhigang Shuai,<sup>c</sup> Daoben Zhu<sup>c</sup> and Ben Zhong Tang<sup>\*ab</sup>

Received (in Cambridge, UK) 25th April 2005, Accepted 23rd May 2005

First published as an Advance Article on the web 14th June 2005

DOI: 10.1039/b505683g

Appending carbazolyl groups to a hexaphenylsilole core yielded thermally and morphologically stable carbazolyloles; the silole carrying two carbazolyl peripheral groups showed photovoltaic activity.

Siloles are a group of wonder molecules that exhibit an array of unusual properties.<sup>1</sup> For example, siloles virtually do not emit when isolated in dilute solutions but emit intensely when aggregated in the solid state, a novel phenomenon for which we coined the term *aggregation-induced emission* (AIE).<sup>2,3</sup> The spectral widths and emission colours of their solid films are narrower and bluer, respectively, than those of their dilute solutions.<sup>4</sup> Furthermore, photoluminescence (PL) spectra of their crystals blue-shift from those of their amorphous films.<sup>5,6</sup> All of these behaviours are opposite to those of “normal” luminophors. Utilizing these unique properties, we developed silole-based visco-, thermo-<sup>3a</sup> and vapochromic systems<sup>6</sup> and constructed silole-based chemo- and biosensors for detecting chemical (*e.g.*, explosives)<sup>5</sup> and biological analytes (*e.g.*, antibodies).<sup>7</sup> We fabricate silole-based light-emitting diodes (LEDs), which emit brilliantly (luminance up to 55880 cd/m<sup>2</sup>)<sup>8</sup> and efficiently (external quantum efficiency up to 8%).<sup>2,9</sup>

Fast electron mobilities have been reported for thin solid films of siloles<sup>4,10</sup> and many groups have used siloles as electron transport materials in the construction of electroluminescence (EL) devices.<sup>11</sup> This fact spurred our interest in using siloles as active materials to construct photovoltaic (PV) cells. Our initial attempts, however, ended with dismay: none of the siloles we tested gave meaningful PV signals. It has been well recognized that excitons dissociate efficiently at a donor (D)–acceptor (A) heterojunction interface.<sup>12–14</sup> Siloles are excellent electron acceptors, because their LUMO levels are lowered by their unique  $\sigma^*-\pi^*$  conjugations.<sup>1,3,11,15</sup> Carbazole (Cz), on the other hand, is a well-known

electron donor and widely used hole transport material. We envisage that introduction of Cz donor groups into the silole acceptor system may create photo-responsive D–A adducts. In this work, we attached Cz group(s) to the 1-position of hexaphenylsilole (HPS; Fig. 1). Whereas the HPS derivative with one Cz group (CzHPS) did not work well as a PV material, its congener with two Cz groups (Cz<sub>2</sub>HPS) exhibited high PV activity.

The Cz moieties are incorporated into the silole structure by desalt coupling: reactions of 1-chloropentaphenylsilole (**1**) and 1,1-dichlorotetraphenylsilole (**2**) with 9-(*p*-lithiobenzyl)carbazole (**3**) yield the HPS derivatives CzHPS and Cz<sub>2</sub>HPS, respectively (Fig. 1), which are thoroughly purified and fully characterized (see ESI for details). While we failed to get a crystal of Cz<sub>2</sub>HPS, a single crystal of CzHPS was grown from a chloroform/acetone mixture, whose crystallographic analysis duly confirmed the structure derived from its spectroscopic data.‡

Thermal stability is an important criterion for evaluating the candidacy of a molecule for optoelectronic applications because of the involvement of thermal processes in the device fabrications and operations. The molecule, for example, needs to be sublimed at high temperatures in the vapour deposition process and experiences repeated annealing by the heat generated when the device is put in use. We investigated the thermal behaviours of the new carbazolyl-siloles using thermal gravimetric analysis (TGA) and differential scanning calorimetry (DSC). TGA analyses reveal that Cz<sub>2</sub>HPS and CzHPS lose 5% of their original weights at 360.4 and

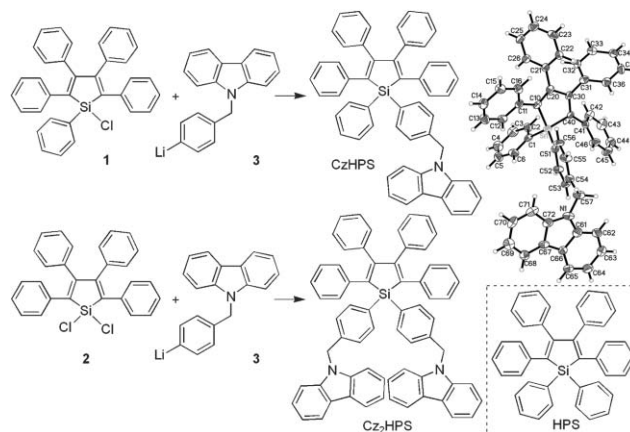


**Fig. 1** Synthesis of Cz<sub>2</sub>HPS's and crystal structure of CzHPS. Molecular structure of their parent form of HPS is given in the inset for reference.

† Electronic supplementary information (ESI) available: preparation and characterization details for CzHPS and Cz<sub>2</sub>HPS, crystallographic data for CzHPS, and fabrication procedures for the LED devices and PV cells. See <http://www.rsc.org/suppdata/cc/b5/b505683g/index.sht>

<sup>a</sup> Department of Chemistry, The Hong Kong University of Science & Technology, Clear Water Bay, Kowloon, Hong Kong, China.

E-mail: tangbenz@ust.hk; Fax: +852-2358-1594; Tel: +852-2358-7375

<sup>b</sup> Department of Polymer Science and Engineering, Zhejiang University, Hangzhou 310027, China

<sup>c</sup> Organic Solids Laboratory, Institute of Chemistry, Chinese Academy of Sciences, Beijing 100080, China

<sup>d</sup> Theoretical Chemistry, Royal Institute of Technology, SCFAB, S-106 91 Stockholm, Sweden

\* tangbenz@ust.hk

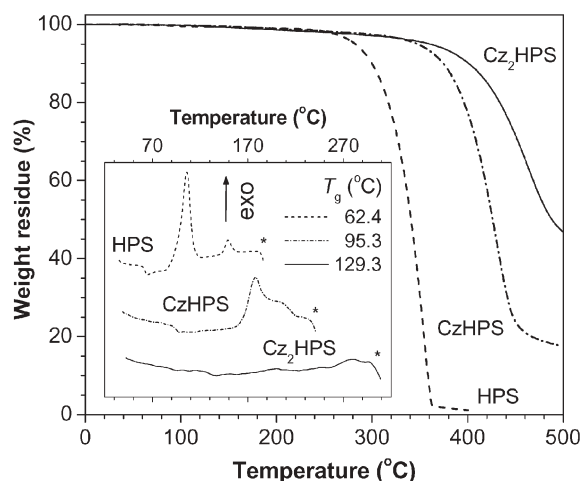


**Fig. 2** TGA and DSC (inset) thermograms of  $\text{Cz}_2\text{HPS}$ 's taken under nitrogen at a heating rate of  $10\text{ }^\circ\text{C}/\text{min}$ , in which the asterisk denotes the start of a melting transition. Data for HPS are shown for comparison.

$347.6\text{ }^\circ\text{C}$ , respectively, while their HPS parent does so at  $282.4\text{ }^\circ\text{C}$  (Fig. 2). Clearly, the introduction of the Cz groups helps enhance the silole's thermal stability.

The Cz groups also help increase HPS's glass ( $T_g$ ) and melting transition temperatures ( $T_m$ ). While  $T_g$  of HPS is  $62.4\text{ }^\circ\text{C}$ , those of CzHPS and  $\text{Cz}_2\text{HPS}$  are much higher, being  $95.3$  and  $129.3\text{ }^\circ\text{C}$ , respectively. Similarly, HPS starts its melting transition from  $182\text{ }^\circ\text{C}$ , but CzHPS and  $\text{Cz}_2\text{HPS}$  do so at  $234$  and  $298\text{ }^\circ\text{C}$ , respectively. Several crystallization transitions are recorded in HPS during the DSC heating scan. These transitions occur in the CzHPS system at higher temperatures, but no such transitions are detectable in the  $\text{Cz}_2\text{HPS}$  system.  $\text{Cz}_2\text{HPS}$  thus enjoys strong thermolytic resistance and high morphological stability.

After studying the thermal transitions of the siloles, we checked their electronic transitions. As shown in Fig. 3A, a CzHPS solution in acetone exhibits two UV peaks at  $331$  and  $345\text{ nm}$ , which are assignable to the absorptions by the Cz and silolyl chromophores, respectively, by comparison with the absorption spectra of  $\text{Cz}^{16}$  and HPS.<sup>3a</sup> When a large amount ( $92\text{ vol}\%$ ) of water, a non-solvent of CzHPS, is added into the acetone solution, the CzHPS molecules aggregate into nanodimensional clusters, as evidenced by the visual transparency of the resultant suspension. The UV spectrum of the nanoaggregates is slightly red-shifted from that of

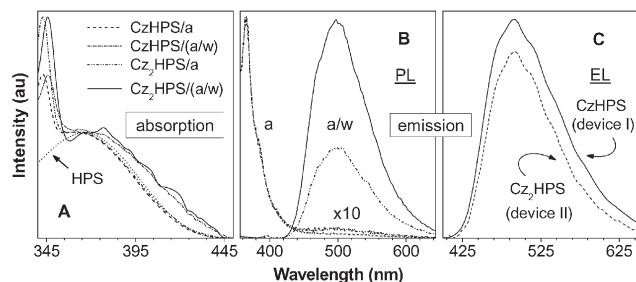


**Fig. 3** (A) Absorption and (B) photoluminescence spectra of  $\text{Cz}_2\text{HPS}$ 's in acetone (a) and an acetone/water (a/w) mixture with  $92\text{ vol}\%$  water; silole concentration:  $0.1\text{--}10\text{ }\mu\text{M}$ ; excitation wavelength:  $345\text{ nm}$ . Data for HPS are shown in (A) for comparison. (C) Electroluminescence spectra of  $\text{Cz}_2\text{HPS}$ -based light-emitting diodes (for device structures, see Note 17).

their isolated species in the dilute solution. A similar phenomenon is observed in the  $\text{Cz}_2\text{HPS}$  system.

The solutions of  $\text{Cz}_2\text{HPS}$ 's in acetone display weak PL spectra peaked at  $366\text{ nm}$ , with very small bumps at  $\sim 498\text{ nm}$  (Fig. 3B). 9-Methylcarbazole emits strongly at  $\sim 364\text{ nm}$  with a quantum yield ( $\eta_{\text{PL}}$ ) of  $51\%$ .<sup>16</sup> The weak emissions of the Cz groups of  $\text{Cz}_2\text{HPS}$ 's at  $366\text{ nm}$  are indicative of intramolecular energy transfer in the dilute solutions: the light emitted from the Cz groups is partially absorbed by the HPS core. The molecularly dissolved HPS species are almost nonemissive,<sup>3a</sup> hence the barely recognizable bumps at  $\sim 498\text{ nm}$ .

Upon addition of a large amount ( $92\%$ ) of water into the silole solutions, the  $\text{Cz}_2\text{HPS}$  molecules cluster into nanoaggregates. The silole emissions at  $\sim 497\text{ nm}$  become much stronger, revealing that  $\text{Cz}_2\text{HPS}$ 's, like their HPS parent, are also AIE-active.<sup>2,3a</sup> The  $\eta_{\text{PL}}$  of the aggregates of CzHPS ( $56\%$ ) is  $\sim 2.4$ -fold higher than that of  $\text{Cz}_2\text{HPS}$  ( $23\%$ ). This suggests that part of the excited singlet state of  $\text{Cz}_2\text{HPS}$  has been quenched through charge dissociation, which is understandable, because the formation of D–A complexes should be a more favorable process in the aggregates of the HPS derivative carrying more Cz units.

We fabricated LEDs using  $\text{Cz}_2\text{HPS}$ 's as the host emitters. The EL spectra of the devices (Fig. 3C) resemble the PL spectra of their nanoaggregates in the acetone/water mixture, confirming that the EL and PL originate from the same species of  $\text{Cz}_2\text{HPS}$  molecules. The EL characteristics of an LED of CzHPS (device I)<sup>17</sup> are shown in Fig. 4A as an example. The device is turned on at  $\sim 5\text{ V}$  and emits with a maximum current efficiency ( $\eta_c$ ) of  $2.6\text{ cd}/\text{A}$  at  $8.5\text{ V}$ . The  $\eta_c$  ( $2.2\text{ cd}/\text{A}$ ) of the LED of  $\text{Cz}_2\text{HPS}$  (device II)<sup>17</sup> is lower than that of CzHPS, in agreement with the trend observed for their  $\eta_{\text{PL}}$ . More excitons may have been annihilated by more efficient charge dissociation in the  $\text{Cz}_2\text{HPS}$  device, because of its

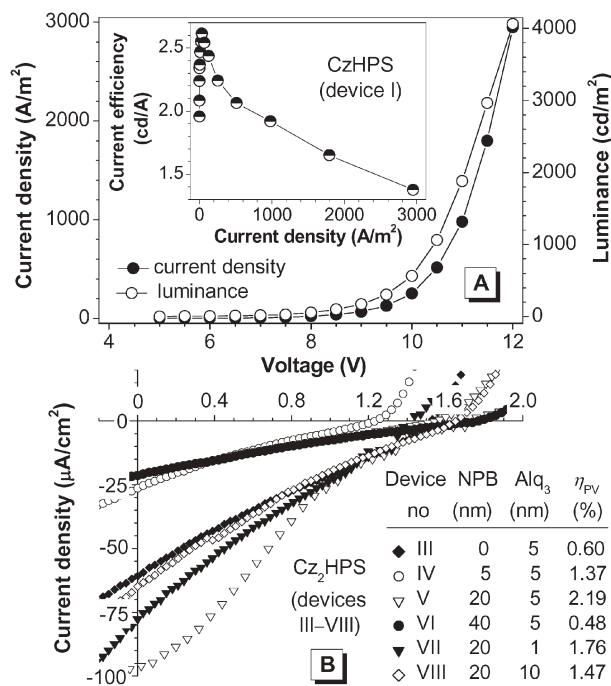


**Fig. 4** (A)  $I$ – $V$ – $L$  and (B)  $I$ – $V$  characteristics of (A) an LED device of CzHPS<sup>17</sup> and (B) PV cells of  $\text{Cz}_2\text{HPS}$ .<sup>18</sup> Inset: current efficiency of the CzHPS-based LED.

higher statistic probability of forming D–A interfaces. This is verified by the result of device III:<sup>18</sup> its  $\eta_C$  is as low as merely 0.018 cd/A.

Efficient charge dissociation at the D–A heterojunction interface is bad for LED but good for PV application and Cz<sub>2</sub>HPS may hence show good PV performance. Under the influence of an applied bias, the dissociated holes and electrons in the respective D and A domains may steadily migrate along the interfaces to corresponding electrodes to finish the PV process of converting light to electricity. We examined the PV responses of the CzHPS- and Cz<sub>2</sub>HPS-based devices (I and II) by shining on them a UV light (365 nm) of low power (15 mW/cm<sup>2</sup>) under applied biases and found their external quantum efficiencies ( $\eta_{PV}$ ) to be 0.14% and 0.27%, respectively. This confirms that Cz<sub>2</sub>HPS is a better PV material than CzHPS.

This conclusion is substantiated by the performance of a series of PV cells of Cz<sub>2</sub>HPS. As can be seen from Fig. 4B, all of the PV cells of Cz<sub>2</sub>HPS (devices III–VIII) show good PV efficiencies. The best results are obtained with device V, whose short-circuit current density, open-circuit voltage, and fill factor are 96.5  $\mu\text{A}/\text{cm}^2$ , 1.7 V, and 0.21, respectively. Although the structure of the cell is far from optimized, it already shows an  $\eta_{PV}$  as high as 2.19%. Optimization of the device structure may further boost the  $\eta_{PV}$  of the Cz<sub>2</sub>HPS-based PV cell.

In summary, in this work, we synthesized Cz<sub>(2)</sub>HPS's comprised of carbazolyl donors and silolyl acceptors. The HPS derivative with two Cz groups, *i.e.* Cz<sub>2</sub>HPS, is thermolytically resistant ( $T_d$  360 °C) and morphologically stable ( $T_g$  129 °C,  $T_m$  298 °C), thanks to the strong D–A interaction in the carbazolylsilole. We have proved the concept that a silole can be made PV-active by attaching donor groups to the silolyl ring. The PV cells of Cz<sub>2</sub>HPS perform well and offer an  $\eta_{PV}$  as high as 2.19%. To our knowledge, these are the first PV cells based on a low molar mass silole. The fact that Cz<sub>2</sub>HPS performs better than CzHPS suggests that introduction of more Cz groups will make silole more photo-responsive. Based on the structural insight gained in this study, we anticipate that an HPS derivative with its silole core fully covered by six Cz peripheral groups will show excellent PV performance. Work along these lines is currently being undertaken in our laboratories.

We are grateful to the Research Grants Council of Hong Kong (603304, 604903, 6085/02P, and 6121/01P), the Natural Science Foundation of China (N\_HKUST606\_03), the Ministry of Science and Technology of China (973 Program), and the Cao Guangbiao Foundation of Zhejiang University.

## Notes and references

† Crystal data for CzHPS: C<sub>53</sub>H<sub>39</sub>NSi,  $M = 717.94$ , monoclinic,  $Cc$ ,  $a = 14.3168(12)$ ,  $b = 14.7242(12)$ ,  $c = 18.7652(15)$  Å,  $\beta = 102.536(2)^\circ$ ,  $V = 3861.5(5)$  Å<sup>3</sup>,  $Z = 4$ ,  $D_c = 1.235$  Mg m<sup>-3</sup>,  $\mu = 0.100$  mm<sup>-1</sup>,  $T = 100(2)$  K,  $2\theta_{\text{max}} = 25.00^\circ$ , 9454 reflections collected, 5093 independent reflections ( $R_{\text{int}} = 0.0537$ ),  $R_1 = 0.0554$  and  $wR_2 = 0.0928$  [ $I > 2\sigma(I)$ ],  $R_1 = 0.0776$  and  $wR_2 = 0.0994$  (all data),  $\Delta e +0.296$  and  $-0.245$  e Å<sup>-3</sup>. CCDC 270218. See <http://www.rsc.org/suppdata/cc/b5/b505683g/index.sht> for crystallographic data in CIF or other electronic format.

1 *e.g.*: (a) H. J. Tracy, J. L. Mullin, W. T. Klooster, J. A. Martin, J. Haug, S. Wallace, I. Rudloe and K. Watts, *Inorg. Chem.*, 2005, **44**, 2003; (b) J. H. Lee, Q. D. Liu, D. R. Bai, Y. J. Kang, Y. Tao and S. N. Wang, *Organometallics*, 2004, **23**, 6205; (c) A. J. Boydston and B. L. Pagenkopf,

- Angew. Chem., Int. Ed.*, 2004, **43**, 6336; (d) J. Ohshita, K. H. Lee, K. Kimura and A. Kunai, *Organometallics*, 2004, **23**, 5622; (e) L. Aubouy, P. Gerbier, N. Huby, G. Wantz, L. Vignau, L. Hirsch and J. M. Janot, *New J. Chem.*, 2004, **28**, 1086; (f) H. Sohn, M. J. Sailor, D. Magde and W. C. Troglor, *J. Am. Chem. Soc.*, 2003, **125**, 3821; (g) I. Touloukhonova, R. P. Zhao, M. Kozee and R. West, *Main Group Met. Chem.*, 2001, **24**, 737.
- 2 (a) J. Luo, Z. Xie, J. W. Y. Lam, L. Cheng, H. Chen, C. Qiu, H. S. Kwok, X. Zhan, Y. Q. Liu, D. B. Zhu and B. Z. Tang, *Chem. Commun.*, 2001, 1740; (b) M. Freemantle, *Chem. Eng. News*, 2001, **79**, 41, 29.
- 3 (a) J. Chen, C. C. W. Law, J. W. Y. Lam, Y. Dong, S. M. F. Lo, I. D. Williams, D. B. Zhu and B. Z. Tang, *Chem. Mater.*, 2003, **15**, 1535; (b) Y. Ren, Y. Q. Dong, J. W. Y. Lam, B. Z. Tang and K. S. Wong, *Chem. Phys. Lett.*, 2005, **402**, 468; (c) Y. Ren, J. W. Y. Lam, Y. Q. Dong, B. Z. Tang and K. S. Wong, *J. Phys. Chem. B*, 2005, **109**, 1135; (d) J. W. Chen, Z. L. Xie, J. W. Y. Lam, C. C. W. Law and B. Z. Tang, *Macromolecules*, 2003, **36**, 1108; (e) B. Z. Tang, X. W. Zhan, G. Yu, P. P. S. Lee, Y. Q. Liu and D. B. Zhu, *J. Mater. Chem.*, 2001, **11**, 2974; (f) C. C. W. Law, J. Chen, J. W. Y. Lam, H. Peng and B. Z. Tang, *J. Inorg. Organomet. Polym.*, 2004, **14**, 39.
- 4 G. Yu, S. Yin, Y. Q. Liu, J. Chen, X. Xu, X. Sun, D. Ma, X. Zhan, Q. Peng, Z. G. Shuai, B. Z. Tang, D. B. Zhu, W. Fang and Y. Luo, *J. Am. Chem. Soc.*, 2005, **127**, 6335.
- 5 Z. Li, Y. Q. Dong, B. Mi, Y. H. Tang, M. Häußler, H. Tong, Y. P. Dong, J. W. Y. Lam, Y. Ren, H. H. Y. Sung, K. S. Wong, P. Gao, I. D. Williams, H. S. Kwok and B. Z. Tang, *J. Phys. Chem. B*, 2005, **109**, 10061.
- 6 Y. Q. Dong, J. W. Y. Lam, Z. Li, H. Tong, Y. P. Dong, X. D. Feng and B. Z. Tang, *J. Inorg. Organomet. Polym. Mater.*, 2005, **15**, 287.
- 7 C. P.-Y. Chan, M. Häußler, B. Z. Tang, Y. Q. Dong, K.-K. Sin, W.-C. Mak, D. Trau, M. Seydack and R. Renneberg, *J. Immunol. Methods*, 2004, **295**, 111.
- 8 (a) H. Chen, J. Chen, C. Qiu, B. Z. Tang, M. Wong and H. S. Kwok, *IEEE J. Sel. Top. Quantum Electron.*, 2004, **10**, 10; (b) J. Chen, H. Peng, C. C. W. Law, Y. Dong, J. W. Y. Lam, I. D. Williams and B. Z. Tang, *Macromolecules*, 2003, **36**, 4319.
- 9 H. Chen, J. W. Y. Lam, J. Luo, Y. Ho, B. Z. Tang, D. B. Zhu, M. Wong and H. S. Kwok, *Appl. Phys. Lett.*, 2002, **81**, 574.
- 10 H. Murata, Z. H. Kafafi and M. Uchida, *Appl. Phys. Lett.*, 2002, **80**, 189.
- 11 *e.g.*: (a) K. Tamao, M. Uchida, T. Izumizawa, K. Furukawa and S. Yamaguchi, *J. Am. Chem. Soc.*, 1996, **118**, 11974; (b) J. Ohshita, K. Kai, A. Takata, T. Iida, A. Kunai, N. Ohta, K. Komaguchi, M. Shiotani, A. Adachi, K. Sakamaki and K. Okita, *Organometallics*, 2001, **20**, 4800.
- 12 (a) J. L. Segura, N. Martin and D. M. Guldi, *Chem. Soc. Rev.*, 2005, **34**, 31; (b) P. Peumans, A. Yakimov and S. R. Forrest, *J. Appl. Phys.*, 2003, **93**, 3693.
- 13 (a) W. U. Huynh, J. J. Dittmer and A. P. Alivisatos, *Science*, 2002, **295**, 2425; (b) L. Schmidt-Mende, A. Fechtenkotter, K. Mullen, E. Moons, R. H. Friend and J. D. MacKenzie, *Science*, 2001, **293**, 1119; (c) G. Yu, J. Gao, J. C. Hummelen, F. Wudl and A. J. Heeger, *Science*, 1995, **270**, 1789.
- 14 (a) B. Z. Tang, H. Z. Chen, R. S. Xu, J. W. Y. Lam, K. K. L. Cheuk, H. N. C. Wong and M. Wang, *Chem. Mater.*, 2000, **12**, 213; (b) J. W. Y. Lam and B. Z. Tang, *J. Polym. Sci., Part A: Polym. Chem.*, 2003, **41**, 2607.
- 15 M. Hissler, P. Dyer and R. Reau, *Coord. Chem. Rev.*, 2003, **244**, 1.
- 16 I. B. Berlman, *Handbook of Fluorescence Spectra of Aromatic Molecules*, Academic Press, New York, 1971.
- 17 Device I: ITO/NPB(700 Å)/CzHPS(200 Å)/Alq<sub>3</sub>(200 Å)/LiF(7 Å)/Al; device II: ITO/NPB(500 Å)/Cz<sub>2</sub>HPS(300 Å)/TPBI(100 Å)/Alq<sub>3</sub>(50 Å)/LiF(7 Å)/Al, where ITO = indium-tin oxide, NPB = *N,N'*-bis(1-naphthyl)-*N,N'*-diphenyl-1,1'-biphenyl-4,4'-diamine, and TPBI = 2,2',2''-(1,3,5-phenylene)tris(1-phenyl-1H-benzimidazole).
- 18 Device III: ITO/NPB(0 Å)/Alq<sub>3</sub>:5% Cz<sub>2</sub>HPS(300 Å)/Alq<sub>3</sub>(50 Å)/LiF(7 Å)/Al; device IV: ITO/NPB(50 Å)/Alq<sub>3</sub>:5% Cz<sub>2</sub>HPS(300 Å)/Alq<sub>3</sub>(50 Å)/LiF(7 Å)/Al; device V: ITO/NPB(200 Å)/Alq<sub>3</sub>:5% Cz<sub>2</sub>HPS(300 Å)/Alq<sub>3</sub>(50 Å)/LiF(7 Å)/Al; device VI: ITO/NPB(400 Å)/Alq<sub>3</sub>:5% Cz<sub>2</sub>HPS(300 Å)/Alq<sub>3</sub>(50 Å)/LiF(7 Å)/Al; device VII: ITO/NPB(200 Å)/Alq<sub>3</sub>:5% Cz<sub>2</sub>HPS(300 Å)/Alq<sub>3</sub>(10 Å)/LiF(7 Å)/Al; device VIII: ITO/NPB(200 Å)/Alq<sub>3</sub>:5% Cz<sub>2</sub>HPS(300 Å)/Alq<sub>3</sub>(100 Å)/LiF(7 Å)/Al.